Proc. Natl. Acad. Sci. USA
Vol. 89, pp. 5705–5709, July 1992
Biochemistry

Cloning, expression, and crystallization of recoverin, a calcium sensor in vision

(retinal rod cell/myristoylation/tryptophan fluorescence/EF hand superfamily/x-ray crystallography)

SANGHAMITRA RAY*†, SERGEY ZOZULYA*‡, GREGORY A. NIEMI§, KEVIN M. FLAHERTY*, DOANE BROLLEY§, ALEXANDER M. DIZHOOR§¶, DAVID B. MCKAY*, JAMES HURLEY§, AND LUBERT STRYER*

*Department of Cell Biology and Beckman Laboratories for Structural Biology, Stanford University School of Medicine, Stanford, CA 94305; §Department of Biochemistry and Howard Hughes Medical Institute, University of Washington, Seattle, WA 98195; ‡Branch of M. M. Shemyakin Institute of Bioorganic Chemistry, Pushchino, Moscow Region, Russia 142292; and ¶A. N. Belozersky Institute of Physico-Chemical Biology, Moscow State University, Moscow, Russia 119899

Contributed by Lubert Stryer, February 26, 1992

ABSTRACT **Recoverin, a recently discovered 23-kDa calcium-binding protein, activates retinal rod guanylate cyclase when the calcium level is lowered in the submicromolar range. We report here the cloning and sequencing of a cDNA for recoverin from a bovine retinal expression library. The recoverin coding sequence was inserted into a pET-11a expression vector under control of the T7 phage promoter. A second expression system, in which the coding sequence was placed under control of the λ phage P_R promoter, gave 10-fold higher yields (10 mg of purified recoverin per liter of *Escherichia coli* culture). The finding that retinal recoverin is myristoylated at its amino terminus led us to coexpress the recombinant protein and *N*-myristoyltransferase (EC 2.3.1.97). Myristoylated recombinant recoverin formed in this way in *E. coli* is like retinal recoverin in exhibiting a large calcium-induced shift in its tryptophan fluorescence emission spectrum. The availability of abundant protein enabled us to crystallize unmyristoylated recombinant recoverin and initiate x-ray studies. The space group of tetragonal crystals obtained from 75% saturation ammonium sulfate is *I*4 with unit cell dimensions $a = 85.1$ Å and $c = 59.8$ Å. These crystals of the calcium-bound form of the protein diffracted to a resolution of 2.2 Å. The expression systems described here open the door to high-resolution x-ray crystallographic and nuclear magnetic resonance studies of this new member of the EF-hand superfamily and to the elucidation of its precise mode of action as a calcium switch.**

Visual excitation in vertebrates is mediated by an enzymatic cascade that lowers the cGMP level and thereby closes membrane channels (for reviews, see refs. 1–6). Restoration of the dark state requires cGMP synthesis by guanylate cyclase. The clue as to how this enzyme is regulated came from electrophysiological studies that revealed a negative feedback loop between cGMP and the cytosolic Ca^{2+} level (7–10). Following illumination, the cytosolic Ca^{2+} concentration decreases markedly, from about 500 to 50 nM. A lowering of the cytosolic Ca^{2+} level in this range stimulates guanylate cyclase about 5-fold in rod outer segment suspensions (11). Activation is mediated by a protein that can be detached from membrane-bound guanylate cyclase. This Ca^{2+}-sensitive stimulatory protein, named recoverin, has recently been purified from bovine retinas (12–14). The amino acid sequence of recoverin (12), a 23-kDa protein, exhibits three potential Ca^{2+}-binding sites (EF hands) (15, 16). Recoverin in fact binds Ca^{2+} as evidenced by $^{45}Ca^{2+}$ blots and the large Ca^{2+}-induced shift in its tryptophan fluorescence emission spectrum. Furthermore, recoverin activates guanylate cyclase in a Ca^{2+}-sensitive manner in rod outer segment membranes depleted of endogenous activator (12, 13).

Interest in recoverin is heightened by the finding that an immunologically cross-reacting protein is present in the pineal gland (12) and in a subpopulation of cone bipolar cells (17). Visinin, a protein isolated from chicken retinal cones (18), is 59% identical in sequence to bovine recoverin. Antibodies to recoverin have been found in sera from patients with cancer-associated retinopathy, a degenerative disease of the retina that is caused by a primary tumor outside the eye (14). The presence of anti-recoverin antibodies in this autoimmune disease suggests that homologs of recoverin may be present in peripheral tissues. Also noteworthy is the recent finding of an ≈26-kDa Ca^{2+}-binding protein in frog retinas that modulates the light-triggered activation of the cGMP phosphodiesterase (19).

We have isolated and sequenced‖ a recoverin cDNA and have developed two high-level expression systems in *Escherichia coli* to facilitate the elucidation of how recoverin acts as Ca^{2+} switch. While these studies were being performed, the N terminus of retinal recoverin was found to be heterogeneously acylated with C_{12} and C_{14} fatty acids (A.M.D., L. H. Ericsson, R. Johnson, S. Kumar, E. Olshevskaya, S.Z., L.S., J.H., and K. A. Walsh, unpublished data). This observation led us to coexpress yeast myristoyltransferase (myristoyl-CoA:protein *N*-myristoyltransferase, EC 2.3.1.97; ref. 21) and recoverin in *E. coli* to form myristoylated recombinant recoverin. The calcium-dependence of the tryptophan emission spectrum of myristoylated and unmyristoylated recombinant recoverin was then compared with that of retinal recoverin. We also report here the initiation of an x-ray crystallographic study of this Ca^{2+} sensor.

MATERIALS AND METHODS

Isolation and Sequencing of Recoverin cDNA. DNA manipulations were carried out by standard methods (22). About ≈6×10^4 phage from a phage λgt11 bovine retina expression library (23) were plated and screened with a 1:4000 dilution of protein A-purified anti-recoverin antibody (12). Purified phage from two independent positive plaques were diluted into distilled water, and the inserts were amplified by PCR using oligonucleotides derived from the *lacZ* sequences bracketing the insert. Two amplified fragments were digested with *Eco*RI endonuclease and ligated into plasmid vector pBS SK(+) (Stratagene) at the *Eco*RI site. They were then used to screen a λgt10 bovine retinal cDNA library (24). Of 4×10^5

The publication costs of this article were defrayed in part by page charge payment. This article must therefore be hereby marked "*advertisement*" in accordance with 18 U.S.C. §1734 solely to indicate this fact.

Abbreviation: IPTG, isopropyl β-D-thiogalactoside.

†Present address: Department of Physiology and Biophysics, University of Washington, Seattle, WA 98195.

‖The sequence reported in this paper has been deposited in the GenBank data base (accession number M77094).

phage screened, 26 independent plaques hybridized with each of these probes. Phage were purified from all 26 plaques. Primer 1 was made to the 5′ noncoding region, and primer 2 was made to the λimm434 region (25) on the 3′ side of the *Eco*RI site bracketing the cDNA insert: 1, GCGGCCGCTGCAGGTCGACGGGCCCACACCACCTCACATATG; 2, AAGCTTGTCGACGGATCCCCAGGGTAAAAAGCAAAA. PCR products from phage isolated from purified positive plaques were probed with the original partial-length clones. Several PCR products were subcloned into the *Sal* I site of pBS SK(+) for sequencing. One of them, named mr21, contained the entire protein coding region.

Construction of Expression Vectors. For expression in *E. coli*, mr21 was inserted into pET-11a (Novagen, Madison, WI) under control of the T7 phage promoter (26) by using the flanking *Nde* I and *Bam*HI sites that were included in the PCR primers used to generate mr21. The host strain for expression was BL21(DE3) containing the pLysS plasmid, which harbors the T7 lysozyme gene (26). This vector will be referred to as pET11a-mr21.

A second expression vector was constructed by recloning recoverin cDNA from pET11a-mr21 into plasmid pTIS1DT (27), which contains the heat-inducible P_R promoter of λ phage. A DNA fragment containing the recoverin coding sequence as well as the gene *10* leader sequence of T7 phage was excised from pET11a-mr21 by digestion with *Xba* I. After the protruding ends were filled by using the Klenow fragment, the fragment was digested with *Bam*HI. The purified fragment was ligated with pTIS1DT vector DNA similarly treated with *Bgl* II, Klenow fragment, and *Bam*HI. This vector will be referred to as pTrec2. Host strains used for its expression were *E. coli* HB101 or DH5α. For coexpressional N-myristoylation of recombinant recoverin, host strain DH5αF′ containing pTrec2 was cotransformed with the compatible plasmid pBB131 carrying the gene for yeast *N*-myristoyltransferase (28).

Expression and Purification of Recoverin. Cells containing pET11a-mr21 were grown in Luria–Bertoni (LB) medium containing chloramphenicol (25 μg/ml) and ampicillin (100 μg/ml) at 37°C and were induced at an A_{600} of 0.6 with 0.4 mM isopropyl β-D-thiogalactoside (IPTG). At an A_{600} of 1.2, cells were collected and pelleted. In the case of pTrec2, the bacterial culture was grown in LB medium with ampicillin (100 μg/ml) at 30–32°C and induced at an A_{600} of 0.6–0.9 by rapidly increasing the temperature to 42°C. For production of myristoylated recoverin, thermal induction of DH5αF′ cells carrying pTrec2 and pBB131 plasmids and grown in LB medium with ampicillin (100 μg/ml), kanamycin (100 μg/ml), and myristic acid (5 mg/ml) was preceded by 30 min of induction with 0.5 mM IPTG. In both cases, after 1–1.5 hr of thermal induction, cells were harvested by centrifugation, suspended in lysis buffer [10 ml of 50 mM Tris·HCl, pH 8.0/1 mM dithiothreitol/5 mM EDTA/10% (vol/vol) glycerol per liter of original bacterial culture], and stored at −70°C.

The harvested biomass was typically processed in batches corresponding to 10–20 liters of original bacterial culture. Two volumes of lysis buffer containing 0.1 mM phenylmethylsulfonyl fluoride was added to the thawed cell slurry. The cells were then disrupted by sonication. Protamine sulfate was added over a 10-min period to a final concentration of 0.1% from a 5% stock prepared in lysis buffer. After stirring for another 10 min, the cell debris was removed by centrifugation at 4°C for 20 min at 10,000 × *g*. Solid ammonium sulfate was added to the cleared lysate with stirring at 4°C to bring it to 60–70% saturation. The precipitate was stirred for 1 hr and removed by centrifugation at 4°C for 20 min at 10,000 × *g*. Supernatant containing recoverin was applied to an 80-ml phenyl-Sepharose CL-4B column (Pharmacia), and the column was washed with 60–70% ammonium sulfate-saturated lysis buffer until proteins were undetectable by the Bradford assay. Fractions containing recoverin were eluted with 150 ml of 20 mM Tris·HCl, pH 8.0/1 mM dithiothreitol/5 mM EGTA/10% glycerol (buffer A) and the eluate was extensively dialyzed against 20 mM Tris·HCl, pH 8.0/1 mM dithiothreitol/2 mM $MgCl_2$/10% glycerol (buffer B). The dialyzed protein solution was applied to an 80-ml Q-Sepharose Fast Flow column and eluted with a gradient of 0–200 mM KCl in buffer B.

Tryptophan Fluorescence Emission Spectra. Spectra were measured on an SLM 8000C spectrofluorimeter (SLM Aminco, Urbana, IL). Samples of 20–200 μg of protein in 2 ml of 40 mM KCl/1 mM $MgCl_2$/2 mM EGTA/80 mM Mops potassium salt, pH 7.1, were titrated by addition of aliquots of 0.1 M $CaCl_2$. Uncorrected fluorescence emission spectra excited at 290 nm at 23°C were recorded from 300 to 400 nm, and a buffer blank was subtracted. The relative sensitivity of the detection system was 1, 0.98, 1.09, 1.13, and 1.46 at 300, 325, 350, 375, and 400 nm, respectively. The maximum increase in volume on addition of Ca^{2+} was 2%. To determine the free Ca^{2+} concentrations of these samples, analogous titrations were carried out in the presence of 1 μM rhod-2 or fluo-3 (Molecular Probes). The fluorescence emission intensities of these indicators were measured, and free Ca^{2+} concentrations were calculated on the basis of K_d values of 0.4 and 1 μM, respectively (29, 30).

X-Ray Crystallography. Crystals of unmyristoylated recombinant recoverin were obtained by the hanging drop/vapor equilibration method (31). Twenty-microliter drops of recombinant recoverin at 10–17 mg/ml in 50 mM Tris·HCl, pH 8.0/1 mM dithiothreitol/1 mM $CaCl_2$/1 mM $MgCl_2$/0.05% sodium azide/35–45% saturated ammonium sulfate were suspended over wells containing the same buffer with double the concentration of ammonium sulfate (70–90% saturation). Crystals formed within 2 weeks at room temperature. They were mounted and sealed in glass x-ray capillaries. Diffraction data were recorded on a Siemens (Iselin, NJ) multiwire area detector interfaced to a Rigaku (Danvers, MA) RU-200 rotating anode x-ray source, with Cu K_α radiation and a 0.2 × 2.0 mm focal spot. Native data were collected from a single crystal by using 0.1° oscillations per frame, 10-cm crystal-to-detector distance, and 20° detector swing. Data were processed with standard programs (32). The space group was determined from the symmetry, and systematic absences were observed in the native data.

RESULTS

Recoverin cDNA Sequence. Two partial-length cDNA clones were obtained by screening a λgt11 bovine retinal cDNA expression library. One of them contained the 5′ noncoding region and the coding region for residues 1–67 of recoverin, and the other encoded residues 76–160. These cDNA clones were used as probes to screen a λgt10 bovine retinal cDNA library for a longer clone. The cDNA inserts in the purified phage DNA of 26 plaques that hybridized to both probes were PCR-amplified. Several of the larger inserts were sequenced (Fig. 1 *Upper*), as was mr21, which encodes the entire protein. The cDNA sequence of recoverin and its deduced amino acid sequence are shown in Fig. 1 *Lower*. This amino acid sequence agrees with that obtained from analyses of partial-length cDNA clones and of peptide fragments of bovine retinal recoverin as reported earlier (12).

Expression and Purification of Unmyristoylated Recombinant Recoverin. *E. coli* harboring pET-11a-mr21 were grown in 12 liters of medium, induced with IPTG, lysed, and treated with protamine sulfate. Chromatography of the soluble fraction on a hydrophobic column (phenyl-Sepharose) followed by chromatography on an ion-exchange column (Q-Sepharose) yielded 10 mg of highly purified protein (Fig. 2, lanes 2–4). An immunoblot showed that recombinant recov-

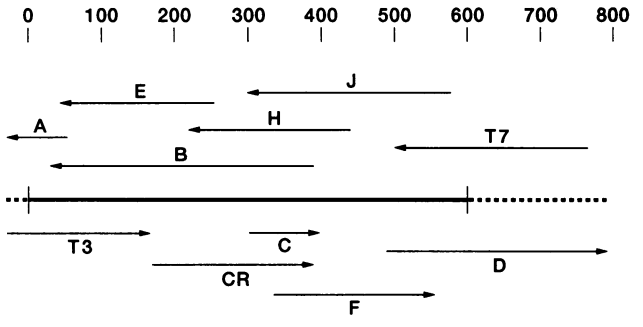


```
  1 CCCGGCCGGGCCCACACCACCTCACCC ATG GGG AAC AGC AAG AGT GGG GCC
                                  M   G   N   S   K   S   G   A
                                  1
 52 CTG TCC AAG GAG ATC CTG GAG GAG CTG CAG CTG AAC ACC AAG TTC
     L   S   K   E   I   L   E   E   L   Q   L   N   T   K   F
         10                                      20
 97 ACG GAG GAG GAG CTG AGC TCC TGG TAC CAG TCC TTC CTG AAG GAG
     T   E   E   E   L   S   S   W   Y   Q   S   F   L   K   E
                             30
142 TGC CCC AGT GGC CGG ATC ACC CGG CAG GAG TTC CAG ACC ATC TAC
     C   P   S   G   R   I   T   R   Q   E   F   Q   T   I   Y
         40                          50
187 TCC AAG TTC TTC CCC GAG GCC GAC CCC AAG GCC TAT GCC CAG CAC
     S   K   F   F   P   E   A   D   P   K   A   Y   A   Q   H
                             60
232 GTG TTC CGA AGC TTT GAT GCC AAC AGC GAT GGC ACC TTG GAC TTC
     V   F   R   S   F   D   A   N   S   D   G   T   L   D   F
         70                                      80
277 AAG GAG TAT GTC ATC GCC TTA CAC ATG ACC AGC GCG GGC AAG ACC
     K   E   Y   V   I   A   L   H   M   T   S   A   G   K   T
                             90
322 AAC CAG AAG CTG GAG TGG GCC TTC TCC CTC TAT GAC GTG GAT GGC
     N   Q   K   L   E   W   A   F   S   L   Y   D   V   D   G
         100                                     110
367 AAT GGG ACC ATC AGC AAG AAC GAA GTG CTG GAG ATT GTC ACG GCT
     N   G   T   I   S   K   N   E   V   L   E   I   V   T   A
                            120
412 ATC TTC AAA ATG ATC AGC CCT GAG GAC ACA AAG CAT CTC CCA GAA
     I   F   K   M   I   S   P   E   D   T   K   H   L   P   E
         130                                     140
457 GAC GAG AAC ACT CCG GAA AAG CGA GCA GAG AAG ATC TGG GGA TTC
     D   E   N   T   P   E   K   R   A   E   K   I   W   G   F
                            150
502 TTT GGC AAG AAG GAT GAT GAT AAA CTT ACA GAG AAA GAA TTC ATC
     F   G   K   K   D   D   D   K   L   T   E   K   E   F   I
         160                                     170
547 GAA GGG ACC CTG GCC AAT AAG GAA ATT CTG CGA CTG ATT CAA TTC
     E   G   T   L   A   N   K   E   I   L   R   L   I   Q   F
                            180
592 GAG CCT CAA AAA GTG AAG GAG AAA CTG AAG GAA AAG AAA CTC TGA
     E   P   Q   K   V   K   E   K   L   K   E   K   K   L   *
             190                                     200
637 TGTCAACTGCTCAGGTCTCCTCCCTCCCCACCCCTCTCAAATAAACACACTTGTGCACG

696 CATG
```

FIG. 1. Sequencing of recoverin cDNA. (*Upper*) Sequencing strategy. Eleven primers (denoted by capital letters) were used to bidirectionally sequence mr21, which encodes the entire amino acid sequence. The arrows show the direction and length of each sequencing reaction. The scale refers to the number of base pairs. (*Lower*) Recoverin cDNA sequence and the corresponding amino acid sequence in single-letter code. The naturally occurring 5′ nontranslated region is shown here; in mr21, this region was modified by PCR for cloning purposes.

erin binds anti-recoverin antibody (Fig. 2, lane 5). A $^{45}Ca^{2+}$ blot showed that the recombinant protein binds Ca^{2+} (Fig. 2, lane 6). N-terminal sequencing showed that the purified protein begins with glycine. Thus, the initiating formylmethionyl group is removed during expression in *E. coli*, in accordance with the known substrate specificity of *E. coli* methionylaminopeptidase (33, 34).

A second expression system was developed to facilitate the production of large amounts of recoverin for structural studies. To this end, a fragment of pET11a-mr21 plasmid DNA containing the complete recoverin coding sequence and a 5′ leader and translation initiation start of phage T7 gene *10* was transferred to the pTIS1DT expression vector (27) and placed under control of the strong heat-inducible P_R promoter of λ phage. Recloning created a translationally coupled two-cistron system (an N-terminal fragment of the phage λ *cro* gene served as the first minicistron), which is known to

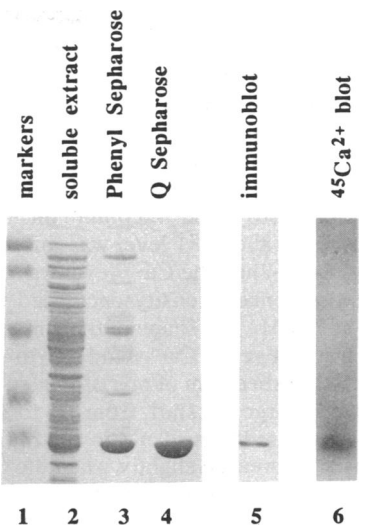

FIG. 2. Purification of recombinant recoverin. In this 12% acrylamide/SDS gel, lane 1 shows prestained molecular mass markers (Bio-Rad) corresponding from top to bottom to 130, 75, 50, 39, and 27 kDa. Lanes: 2–4, soluble extract from *E. coli*, the low-salt eluate from a phenyl-Sepharose column, and the peak fraction from a Q-Sepharose column, respectively; 5, immunoblot of the peak fraction with anti-recoverin antibody; 6, autoradiogram of a $^{45}Ca^{2+}$ blot of the peak fraction.

improve the expression of most target genes (35, 36). The higher yield with the pTrec2 expression system (7–12 mg of purified recoverin per liter of culture) than with the pET11a-mr21 system (1 mg per liter) is probably due to more efficient initiation of translation with pTrec2. Recoverins produced by the two expression systems are indistinguishable on the basis of amino acid analysis and sequencing of the first 10 residues.

Expression and Purification of Myristoylated Recombinant Recoverin. Recombinant myristoylated recoverin was produced by coexpressing recoverin and *Saccharomyces cerevisiae* myristoyl-CoA:protein *N*-myristoyltransferase in *E. coli*. This enzyme catalyzes cotranslational attachment of a myristoyl group (C14:0) to the N-terminal glycine residue of proteins containing appropriate recognition sequences (21). Expression of both proteins was achieved by cotransformation of *E. coli* with the recoverin expression vector pTrec2 described above and the compatible plasmid pBB131 (28) carrying the gene for *N*-myristoyltransferase controlled by the *tac* promoter. Synthesis of *N*-myristoyltransferase induced by IPTG is independent of recoverin synthesis induced by a rise in temperature, allowing temporal control of coexpression. This double plasmid approach has been advantageously used to myristoylate a number of recombinant proteins in *E. coli* (21, 28, 37, 38). To determine whether recoverin was myristoylated, [9,10-^{3}H]myristic acid (39.3 Ci/mmol, 50 μCi/ml of culture; 1 Ci = 37 GBq) was added to bacterial cultures immediately before thermal induction, and total cell lysates were analyzed by SDS/polyacrylamide gel electrophoresis and fluorography. The electrophoretic mobility of the major radiolabeled band corresponded to that of recoverin; its presence was dependent on induction of NMT synthesis. Several minor higher molecular weight bands, presumably myristoylated endogenous *E. coli* proteins (28, 37), were also observed.

Myristoylated recombinant recoverin was isolated with similar yield and behaved like its unmodified counterpart during the purification procedure except that it was eluted from a Q-Sepharose column at higher ionic strength (≈120 mM KCl versus 80 mM, in the absence of Ca^{2+}). Ca^{2+} lowered the ionic strength required for elution of both the unmyristoylated and myristoylated forms of recombinant

recoverin. The isoelectric point of the unmyristoylated protein is 5.6, compared with 5.1 for the myristoylated recombinant protein and native retinal recoverin.

Ca^{2+} Binding by Recoverin. The tryptophan fluorescence emission spectrum of the recombinant recoverins was measured and compared with that of the native protein, which had been shown to be Ca^{2+}-sensitive (12). The fluorescence intensity of unmyristoylated recombinant recoverin increased slightly when the Ca^{2+} level was raised from 70 nM to 400 nM (Fig. 3*A*). When the Ca^{2+} level was then raised to 10 μM, the fluorescence intensity decreased to nearly the same value as at 70 nM. The shape of the emission spectrum was virtually insensitive to Ca^{2+} binding. In contrast, the tryptophan emission spectrum of myristoylated recombinant recoverin showed a large red shift, from 333 to 339 nm, when the Ca^{2+} level was raised from 70 nM to 10 μM (Fig. 3*B*). The emission intensity decreased slightly when the Ca^{2+} concentration was raised in several increments from 70 nM to 700 nM. Further addition of Ca^{2+} led to a pronounced red shift and a concomitant decrease in intensity. The Ca^{2+}-dependence of the emission spectrum of myristoylated recombinant recoverin is virtually identical to that of retinal recoverin (Fig. 3*C*).

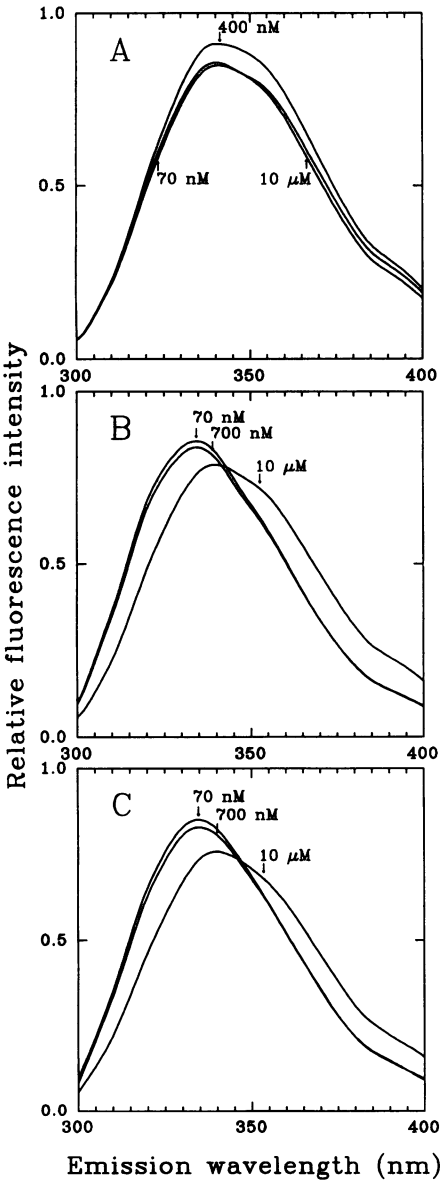

FIG. 3. Effect of the addition of Ca^{2+} on the tryptophan fluorescence emission spectrum of unmyristoylated recombinant recoverin (*A*), myristoylated recombinant recoverin (*B*), and retinal recoverin (*C*)—all excited at 290 nm. The free Ca^{2+} concentration is shown next to each spectrum.

X-Ray Studies of Recombinant Recoverin. Crystals obtained from 70–90% saturation ammonium sulfate are tetragonal, space group *I*4, with unit cell dimensions $a = 85.1$ Å and $c = 59.8$ Å. Ca^{2+} was bound to recoverin in these crystals because the Ca^{2+} concentration of the crystallization medium was 1 mM. The unit cell contains eight asymmetric units. One recoverin protomer per asymmetric unit would give a volume of 2.4 Å^3/Da of protein, which is well within the range of typical values of this parameter for protein crystals (39). Diffraction to 2.2 Å is clearly evident on still and oscillation frames recorded on a Siemens multiwire area detector. A complete set of native data was collected to 2.2 Å resolution from one crystal; the merging *R* factor for symmetry-related reflections was 0.038.

DISCUSSION

We have cloned, sequenced, and expressed a cDNA for bovine recoverin. The cDNA sequence shown in Fig. 1 *Lower* is identical to the recently published sequence of the cDNA for bovine retinal p26 (40) except for three nucleotide changes in the coding region (T296C, A391G, and C358T; nucleotides numbered according to Fig. 1 *Lower*), which were seen in two independently derived PCR products. These differences do not alter the amino acid sequence of recoverin. They probably are due to genetic heterogeneity rather than to PCR errors. The availability of the cDNA enabled us to develop a high-yield expression system in *E. coli*. The pTrec2 system, which uses the λ phage P_R promoter, provides about 10 mg of purified recoverin per liter of culture. A puzzling initial finding was that the Ca^{2+} dependence of the tryptophan fluorescence spectrum of recombinant recoverin differs from that of retinal recoverin (Fig. 3 *A* versus *C*). We then learned that retinal recoverin contains a myristoyl or related fatty acyl group at its N terminus (20). This finding led us to coexpress recoverin with yeast myristoyltransferase (28). The resulting recombinant protein is in fact quantitatively myristoylated, as evidenced by the incorporation of tritiated myristic acid, the shift in isoelectric point to that of retinal recoverin, and mass spectrometric analysis (A.M.D., L. H. Ericsson, R. Johnson, S. Kumar, E. Olshevskaya, S.Z., L.S., J.H., and K. A. Walsh, unpublished data).

Recoverin contains a consensus sequence for myristoylation. The presence of glycine at position 2 of the nascent protein assures cleavage of the initiating methionine residue. The resulting N-terminal glycine is essential for myristoylation (21). N-terminal acylation is also favored by the presence of an uncharged residue (asparagine) at residue 2 of the mature protein and of serine at position 5. Likewise, chicken visinin (18), which is 59% identical to recoverin, contains a myristoylation consensus sequence. Calcineurin B (the Ca^{2+}-binding subunit of protein phosphatase B), which is 27% identical in sequence to recoverin, is also myristoylated (20).

The fluorescence emission of recoverin, which comes from tryptophans 31, 104, and 156, is responsive to both myristoylation and the binding of Ca^{2+} (Fig. 3). In the absence of Ca^{2+}, the emission maximum is at 333 nm for the retinal and myristoylated recombinant proteins and at 339 nm for unmyristoylated recoverin. Myristoylation makes the environment of one or more tryptophans less polar, either by directly shielding the indole ring from water or by inducing a conformational change that has the same effect. At a high Ca^{2+} level the emission spectra of the myristoylated and unmyristoylated proteins are very similar. The emission intensity of unmyristoylated recoverin increases and then decreases on addition of Ca^{2+} in the submicromolar range, indicating that

the protein contains at least two Ca^{2+}-binding sites. Likewise, the Ca^{2+} dependence of the emission spectrum of the myristoylated protein points to the existence of multiple Ca^{2+}-binding sites, as was inferred from the amino acid sequence (12). Studies of the effect of unmyristoylated and myristoylated recombinant recoverins on guanylate cyclase activity are in progress.

The availability of large quantities of recoverin enabled us to crystallize the Ca^{2+}-bound form of the unmyristoylated protein. These crystals diffract to 2.2 Å, indicating that they are suitable for high-resolution structural study. Also, a well-resolved proton NMR spectrum was obtained from a solution (35 mg/ml) of the unmyristoylated protein. Structural studies are needed of the Ca^{2+}-free and Ca^{2+}-bound forms of the myristoylated protein to learn how N-terminal fatty acylation modifies the protein and how recoverin acts as a Ca^{2+} switch. A well-defined system for the reconstitution of regulated guanylate cyclase activity will also be needed to elucidate the precise mechanism of action of recoverin.

We thank Dan Chasman for valuable advice on expression vectors, David Lawlor for helpful discussions on cloning strategies, Jeffrey Gordon for a gift of the *N*-myristoyltransferase cDNA, and Dan Oprian and Jeremy Nathans for kindly providing us with retinal cDNA libraries. This work was supported by grants from the National Eye Institute (EY06641 to J.H. and EY02005 to L.S.) and the National Institute of General Medical Sciences (GM24032 to L.S.).

1. Stryer, L. (1991) *J. Biol. Chem.* **266,** 10711–10714.
2. McNaughton, P. A. (1990) *Physiol. Rev.* **70,** 847–883.
3. Chabre, M. & Deterre, P. (1989) *Eur. J. Biochem.* **179,** 255–266.
4. Baylor, D. A. (1987) *Invest. Ophthalmol. Visual Sci.* **28,** 34–49.
5. Liebman, P. A., Parker, K. R. & Dratz, E. A. (1987) *Annu. Rev. Physiol.* **49,** 765–791.
6. Hurley, J. B. (1987) *Annu. Rev. Physiol.* **49,** 793–812.
7. Yau, K. W. & Nakatani, K. (1985) *Nature (London)* **313,** 579–582.
8. Matthews, H. R., Torre, V. & Lamb, T. D. (1985) *Nature (London)* **313,** 582–585.
9. McNaughton, P. A., Cervetto, L. & Nunn, B. J. (1986) *Nature (London)* **322,** 261–263.
10. Cervetto, L., Lagnado, L., Perry, R. J., Robinson, D. W. & McNaughton, P. A. (1989) *Nature (London)* **337,** 740–743.
11. Koch, K. W. & Stryer, L. (1988) *Nature (London)* **334,** 64–66.
12. Dizhoor, A. M., Ray, S., Kumar, S., Niemi, G., Spencer, M., Brolley, D., Walsh, K. A., Philipov, P. P., Hurley, J. B. & Stryer, L. (1991) *Science* **251,** 915–918.
13. Lambrecht, H. G. & Koch, K. W. (1991) *EMBO J.* **10,** 793–798.
14. Polans, A. S., Buczylko, J., Crabb, J. & Palczewski, K. (1991) *J. Cell. Biol.* **112,** 981–989.
15. Persechini, A., Moncrief, N. D. & Kretsinger, R. H. (1989) *Trends Neurosci.* **12,** 462–467.
16. Strynadka, N. C. J. & James, M. N. G. (1989) *Annu. Rev. Biochem.* **58,** 951–998.
17. Bunt-Milam, A. H., Dacey, D. & Dizhoor, A. M. (1991) *Invest. Ophthalmol. Visual Sci.* **32,** 1264.
18. Yamagata, K., Goto, K., Kuo, C. H., Kondo, H. & Miki, N. (1990) *Neuron* **4,** 469–476.
19. Kawamura, S. & Murakami, M. (1991) *Nature (London)* **349,** 420–423.
20. Aitken, A., Cohen, P., Santikarn, S., Williams, D. H., Calder, A. G., Smith, A. & Klee, C. B. (1982) *FEBS Lett.* **150,** 314–318.
21. Gordon, J. I., Duronio, R. J., Rudnick, D. A., Adams, S. P. & Gokel, G. W. (1991) *J. Biol. Chem.* **266,** 8647–8650.
22. Sambrook, J., Maniatis, T. & Fritsch, E. F. (1989) *Molecular Cloning: A Laboratory Manual* (Cold Spring Harbor Lab., Cold Spring Harbor, NY), 2nd Ed.
23. Yatsunami, K., Pandya, B. V., Oprian, D. D. & Khorana, H. G. (1985) *Proc. Natl. Acad. Sci. USA* **82,** 1936–1940.
24. Nathans, J. & Hogness, D. S. (1983) *Cell* **34,** 807–814.
25. Kuziel, W. A. & Tucker, P. W. (1987) *Nucleic Acids Res.* **15,** 3181.
26. Studier, F. W., Rosenberg, A. H., Dunn, J. J. & Dubendorff, J. W. (1990) *Methods Enzymol.* **185,** 60–89.
27. Skiba, N. P., Udovichenko, I. P., Bondarenko, V. A., Natochin, M. Y., Yurovskaya, A. A., Zozulya, S. A., Shirokova, E. P. & Lipkin, V. M. (1990) *Biol. Membr.* **7,** 230–242.
28. Duronio, R. J., Jackson, M. E., Heuckeroth, R. O., Olins, P. O., Devine, C. S., Yonemoto, W., Slice, L. W., Taylor, S. S. & Gordon, J. I. (1990) *Proc. Natl. Acad. Sci. USA* **87,** 1506–1510.
29. Minta, A., Kao, J. P. & Tsien, R. Y. (1989) *J. Biol. Chem.* **264,** 8171–8178.
30. Tsien, R. Y. & Pozzan, T. (1989) *Methods Enzymol.* **172,** 230–262.
31. McPherson, A. (1976) *Methods Biochem. Anal.* **23,** 249–345.
32. Kabsch, W. J. (1988) *J. Appl. Crystallogr.* **21,** 916–924.
33. Hirel, P. H., Schmitter, M. J., Dessen, P., Fayat, G. & Blanquet, S. (1989) *Proc. Natl. Acad. Sci. USA* **86,** 8247–8251.
34. Huang, S., Elliott, R. C., Liu, P.-S., Koduri, R. K., Weickmann, J. L., Lee, J.-H., Blair, L. C., Ghosh-Dastidar, P., Bradshaw, R. A., Bryan, K. M., Einarson, B., Kendall, R. L., Kolacz, K. M. & Saito, K. (1987) *Biochemistry* **26,** 8242–8246.
35. Schoner, B. E., Belagaje, R. M. & Schoner, R. G. (1986) *Proc. Natl. Acad. Sci. USA* **83,** 8506–8510.
36. Schoner, B. E., Belagaje, R. M. & Schoner, B. G. (1990) *Methods Enzymol.* **185,** 94–103.
37. Duronio, R. J., Rudnick, D. A., Adams, S. P., Towler, D. A. & Gordon, J. I. (1990) *J. Biol. Chem.* **266,** 10498–10504.
38. Linder, M. E., Pang, I.-H., Duronio, R. J., Gordon, J. I., Sternweis, P. C. & Gilman, A. G. (1991) *J. Biol. Chem.* **266,** 4654–4659.
39. Matthews, B. W. (1968) *J. Mol. Biol.* **33,** 491–497.
40. Kutuzov, M. A., Shmukler, B. E., Suslov, O. N., Dergachev, A. E., Zargarov, A. A. & Abdulaev, N. G. (1991) *FEBS Lett.* **293,** 21–24.